JCTC Journal of Chemical Theory and Computation

Electronic Excitations of Simple Cyanine Dyes: Reconciling Density Functional and Wave Function Methods

Robert Send,*,† Omar Valsson,*,‡ and Claudia Filippi*,‡

Institut für Physikalische Chemie, Karlsruher Institut für Technologie, Kaiserstraβe 12, 76131 Karlsruhe, Germany, and Faculty of Science and Technology and MESA+ Research Institute, University of Twente, P.O. Box 217, 7500 AE Enschede, The Netherlands

Received November 3, 2010

Abstract: The simplest cyanine dye series $[H_2N(CH)_nNH_2]^+$ with $n = 1$, 3, 5, 7, and 9 appears to be a challenge for all theoretical excited-state methods since the experimental spectra are difficult to predict and the observed deviations cannot be easily explained with standard arguments. We compute here the lowest vertical excitation energies of these dyes using a variety of approaches, namely, complete active space second-order perturbation theory (CASPT2), quantum Monte Carlo methods (QMC), coupled cluster linear response up to third approximate order (CC3), and various flavors of time-dependent density functional theory (TDDFT), including the recently proposed perturbative correction scheme (B2PLYP). In our calculations, all parameters such as basis set, active space, and geometry dependence are carefully analyzed. We find that all wave function methods give reasonably close excitation energies, with CASPT2 yielding the lowest values, and that the B2PLYP scheme gives excitations in satisfactory agreement with CC3 and DMC, significantly improving on the generalized gradient and hybrid approximations. Finally, to resolve the remaining discrepancy between predicted excitation energies and experimental absorption spectra, we also investigate the effect of excited-state relaxation. Our results indicate that a direct comparison of the experimental absorption maxima and the theoretical vertical excitations is not possible due to the presence of nonvertical transitions. The apparent agreement of earlier CASPT2 calculations with experiments was an artifact of the choice of active space and the use of an older definition of the zero-order Hamiltonian.

1. Introduction

Cyanine dyes are characterized by a conjugated π-electron system connecting two nitrogen atoms and carrying a positive charge.[1] They are naturally occurring as red colorants in fly agaric mushrooms or red beets[2] and are of great industrial interest for their application in solar cells,[3] optical storage media (CDs, DVDs),[4] cancer cell recognition,[5] nonlinear optics,[6] and as biomarkers for nucleic acid detection.[7] This wide range of important applications has made cyanine dyes an early target of theoretical studies aimed at demonstrating the predictive power of computational approaches.[8]

In the past two decades, efficient computational approaches for excited states have been developed, which allow the description of large dyes and the fast screening of molecular libraries in search of specific excited-state properties.[9] In particular, time-dependent density functional theory (TDDFT)[10−12] has become the method of choice for the study of large molecular systems and has been successfully employed to search for highly specialized chromophores and investigate several dye

* E-mail: robert.send@kit.edu; o.valsson@utwente.nl; c.filippi@utwente.nl.

† Karlsruher Institut für Technologie.

‡ University of Twente.

10.1021/ct1006295
Published on Web 01/10/2011

families.[13,14] The efficiency of TDDFT comes in some cases at the price of lower accuracy as compared to conventional highly correlated quantum chemistry methods. It is, for instance, well-known that the description of excitations with charge-transfer, multireference, or Rydberg character is generally problematic in TDDFT. Since none of these features appears to characterize the lowest excited state of the cyanine dyes, one would expect TDDFT to be well suited for the description of this class of systems.

Surprisingly, as early as 2001, Schreiber et al.[15] showed that the excitation energies of the cyanine dyes obtained by TDDFT deviate by more than 1 eV from the values obtained with the CASPT2 method, which is often regarded as one of the most accurate excited-state approaches available. Since the examples chosen in ref 15 were the simplest models of cyanine dyes, the result suggests that TDDFT is not applicable to any member of this dye family. Until today, none of the available density functionals significantly improved the agreement with the reference CASPT2 values given in ref 15. The reasons for the large errors in the TDDFT results for the cyanine dyes are not understood.

Since the early work by Schreiber et al.,[15] excited-state methods have seen several important developments: (i) The efficient implementation of coupled-cluster (CC) response methods in combination with the resolution-of-the-identity (RI) approximation represents a powerful single-reference complement to TDDFT,[16] (ii) Efficient excited-state gradient methods render a large number of excited-state properties accessible.[17,18] (iii) Developments in algorithms and hardware allow for the use of larger basis sets and higher-level theories. (iv) Quantum Monte Carlo (QMC) methods can be used as an alternative to CASPT2 and independent validation of TDDFT.[19−22] (v) The CASPT2 method has been modified and generally improved by the introduction of a novel definition of the zeroth-order Hamiltonian.[23]

None of these developments have been fully exploited in recent calculations of the cyanine dyes, where most efforts have instead been directed to apply different flavors of density functionals in order to improve the excitations and gain insight into the shortcomings of TDDFT. Unfortunately, none of the used functionals has yielded significant improvement, and the insight gained has therefore been limited. The only exception is the B2PLYP scheme by Grimme, which incorporates a perturbative correction based on Kohn−Sham orbitals in a form similar to wave function treatments.[24,25] We note that the extensive excitation benchmark of wave function methods of ref 26 unfortunately does not include any member of the cyanine dye family.

The present work represents a comprehensive treatment of the simple cyanine dye series using several state-of-the-art excited-state methods such as CASPT2, QMC, and CC response methods up to third approximate order; TDDFT also in the long-range corrected and B2PLYP flavors; and the Tamm−Dancoff approximation. We give a detailed account of all parameters which may affect the calculation of the excitations in the various approaches. Our discussion focuses on the lowest bright excited state, and we enclose results for higher excited states in the Supporting Information.

All computational details are given in section 2. We describe the dependence of the excitation energies on the basis set and the method used to optimize the ground-state geometry in section 3.1. This is followed by the excitation energies calculated with CC methods (section 3.2), CASPT2 (section 3.3), QMC (section 3.4), and TDDFT (section 3.5). In section 4, we discuss the relative performance of the theoretical approaches and their comparison with experiments. Our conclusions are summarized in section 5.

2. Computational Details

The ground-state structures are optimized within Hartree−Fock (HF), second-order Møller−Plesset (MP2), and density functional theory (DFT). To compute the excitation energies, we employ coupled-cluster (CC) methods, time-dependent density functional theory (TDDFT), the complete active space self-consistent field (CASSCF) method with its perturbative extension (CASPT2), and quantum Monte Carlo (QMC) methods. The CC response calculations[27,28] are performed at the singles (CCS), singles and doubles (CCSD),[29] approximate second (CC2),[16,30−32] and approximate third (CC3)[33,34] orders. In the DFT calculations, the PBE,[35] PBE0,[36−38] CAM-B3LYP,[39] and B2PLYP[24,25] functionals are employed. The Tamm−Dancoff approximation is employed in some of the TDDFT calculations and denoted with the prefix TDA.[40]

The resolution-of-the-identity (RI) approximation[41] is used in all MP2 and in some CC2 calculations and is indicated by the abbreviations RI-MP2[42] and RI-CC2.[31] All RI-MP2, RI-CC, and DFT calculations are performed with the TURBOMOLE code.[43] B2PLYP calculations are based on an unreleased TURBOMOLE implementation and the additional on top program RICC by Grimme.[24,25] The CC and CAM-B3LYP excitation energies calculated without the RI approximation are obtained with the DALTON program suite.[44] The CAM-B3LYP excitation energy of the largest dye with the triple-ζ basis is computed with the Gaussian 09 code.[45]

The complete active space calculations are performed using MOLCAS 7.2.[46] In the CASPT2 calculations, we employ the default IPEA zero-order Hamiltonian[23] unless otherwise stated and indicate if an additional constant level shift[47] is added to the Hamiltonian. In the CASPT2 calculations, we do not correlate as many of the lowest σ orbitals, as there are heavy atoms in the molecule. For some models, we use the Cholesky decomposition of the two-electron integrals[48] with the threshold of 10^{-8}. The default convergence criteria are used for all calculations.

The program package CHAMP[49] is used for the QMC calculations. We employ scalar-relativistic energy-consistent Hartree−Fock pseudopotentials[50] where the carbon and nitrogen 1s electrons are replaced by a nonsingular s−nonlocal pseudopotential and the hydrogen potential is softened by removing the Coulomb divergence. Different Jastrow factors are used to describe the correlation with different atom types, and for each atom type, the Jastrow factor consists of an exponential of the sum of two fifth-order polynomials of the electron−nucleus and the electron−electron distances, respectively.[51] We also test the effect of including an

electron−electron−nuclear term. The starting determinantal components are obtained in CASSCF calculations, which are performed with the program GAMESS(US),[52] and the final CAS expansions are expressed on the CASSCF natural orbitals. The CAS wave functions of the states of interest may be truncated with an appropriate threshold on the CSF coefficients for use in the QMC calculations. The Jastrow correlation factor and the CI coefficients are optimized by energy minimization within VMC, and when indicated in the text, also the orbitals are optimized along with the Jastrow and CI parameters. The pseudopotentials are treated beyond the locality approximation,[53] and an imaginary time step of 0.05 au is used in the DMC calculations.

2.1. Basis Sets and Ground-State Structures. To investigate the basis-set dependence of the ground-state structures and of the CC and TDDFT excitations, we use the ANO-L-VXZP basis sets[54] and Dunning's correlation consistent cc-pVXZ and aug-cc-pVXZ basis sets.[55−58] For the ANO basis sets, the MOLCAS contraction scheme is employed, namely, ANO-L-VDZP [3s2p1d]/[2s1p], ANO-L-VTZP [4s3p2d1f]/[3s2p1d], and ANO-L-VQZP [5s4p3d2f]/[4s3p1d]. The ANO-L-VXZP series is used in the CASSCF and CASPT2 calculations.

In the QMC calculations, we use the Gaussian basis sets[50] specifically constructed for our pseudopotentials. In particular, we employ the cc-pVDZ basis, denoted by D, and the T′ and Q′ basis sets, which consist of the cc-pVDZ for hydrogen combined respectively with the cc-pVTZ and cc-pVQZ basis sets for the heavy atoms. The D+, T′+, and Q′+ basis sets are constructed by augmenting the corresponding basis with diffuse s, p, and d functions[59] on the heavy atoms. Basis functions with higher angular momentum than d are not included in the T′, T′+, Q′, and Q′+ basis sets.

Unless indicated otherwise, the CC, CASPT2, and TDDFT excitation energies are calculated with the ANO-L-VTZP basis set and the QMC excitations with the T′+ basis set. All excitation energies are computed on the RI-MP2/cc-pVQZ ground-state structures with the exception of the TDDFT excitations, which are obtained using the PBE0/cc-pVQZ structures.

2.2. Auxiliary Basis Sets. In the RI-MP2/ANO-L-VXZP and RI-CC2/ANO-L-VXZP calculations, the corresponding auxiliary basis sets are not available. To assess the impact of using the ANO-L-VXZP basis sets in combination with the available aug-cc-pVXZ auxiliary basis sets, we calculate the error in the correlation energy introduced by the RI approximation for carbon and nitrogen atoms and for H_2. The quantity commonly used to access the quality of an auxiliary basis set is defined as

$$\alpha = \frac{\delta_{\mathrm{RI}}}{|\Delta E(\mathrm{MP2})|} \tag{1}$$

where ΔE(MP2) is the MP2 correlation energy and δ_{RI} is given by

$$\delta_{\mathrm{RI}} = \frac{1}{4}\sum_{i<j}^{\mathrm{occ.}}\sum_{a<b}^{\mathrm{virt.}} \frac{\left|\langle ab||ij\rangle_{\mathrm{exact}} - \langle ab||ij\rangle_{\mathrm{RI}}\right|^2}{\varepsilon_a - \varepsilon_i + \varepsilon_b - \varepsilon_j} \tag{2}$$

The values of α obtained by combining the ANO-L-VXZP basis with the auxiliary aug-cc-pVXZ basis sets are given in the Supporting Information. When the aug-cc-pVQZ auxiliary basis is employed, $\alpha < 0.05$ ppm, which is in line with standard auxiliary-basis-optimization conditions.[58] Therefore, we adopt this auxiliary basis in all of our RI calculations.

2.3. Extrapolation of Excitation Energies. The extrapolated CC3/ANO-L-VTZP (exCC3) excitation energies are obtained as

$$\tilde{E}_{\mathrm{T}}^{\mathrm{CC3}} = E_{\mathrm{T}}^{\mathrm{CC2}} + (E_{\mathrm{D}}^{\mathrm{CC3}} - E_{\mathrm{D}}^{\mathrm{CC2}}) \tag{3}$$

This extrapolation formula is motivated by the observation that triple excitations are less basis-set-sensitive than single and double excitations.[60−62]

3. Vertical Excitation Energies

The cyanine dye molecules studied in this work are shown in Figure 1. We consider hydrogen-terminated dyes of increasing size, which we denote as CN3, CN5, CN7, CN9, and CN11. All hydrogen-terminated dyes have C_{2v} symmetry. For these molecules, we also construct the equivalent dyes where the terminating hydrogens are substituted by methyl groups.

3.1. Basis Set Convergence and Geometry Dependence. We employ the cc-pVXZ, aug-cc-pVXZ, and ANO-L-VXZP series to investigate the basis set dependence of the CC and CASPT2 excitations and give a complete survey of the results in the Supporting Information (SI). In this section, we focus on the smallest molecule, CN3, since it displays the largest dependence on the basis set. The basis-set dependence of the TDDFT and QMC excitations will be discussed separately.

The CC2 excitations of CN3 as a function of the basis set are shown in Figure 2. The correlation-consistent basis series gives the slowest convergence in the excitation energy as a function of basis set size, and an error which is still as large as 0.15 eV when a quadruple-ζ basis is employed. The inclusion of augmentation completely cures the problem since the energy obtained with the double-ζ basis only differs from the augmented quadruple-ζ value by 0.02 eV. The excitations computed with the ANO series converge similarly to the augmented correlation consistent values, and the use of a triple-ζ basis yields the quadruple-ζ value within better than 0.01 eV.

The behavior of the CASPT2 excitations as a function of the basis set is shown for CN3 in Figure 3. The excitations are obtained with the standard IPEA Hamiltonian (S-IPEA) as well as with the IPEA shift set to zero (0-IPEA), as in versions of MOLCAS prior to 6.4. The energies obtained with the IPEA Hamiltonian are 0.2 eV higher than the values obtained without the shift, and the difference is independent of the choice of the basis set. The behavior of the CASPT2 values with and without the IPEA shift closely parallels what is observed for the CC2 excitations. In particular, the inclusion of diffuse augmentation is absolutely necessary

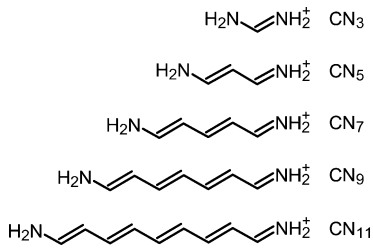

Figure 1. Hydrogen-terminated cyanine dyes considered in this work. Only one of the two resonant structures of each molecule is shown. The other structure can be obtained by having the first double bond at the other nitrogen atom.

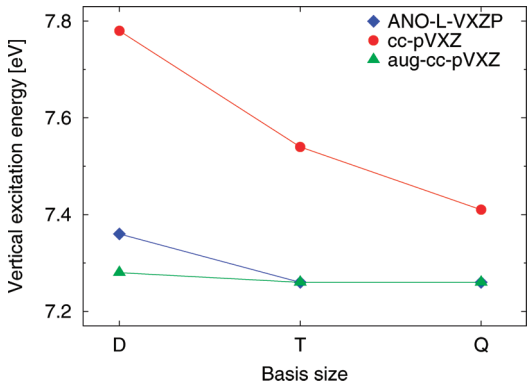

Figure 2. CC2 vertical excitation energies of CN3 computed with different basis sets. The ground-state MP2/cc-pVQZ geometry is used.

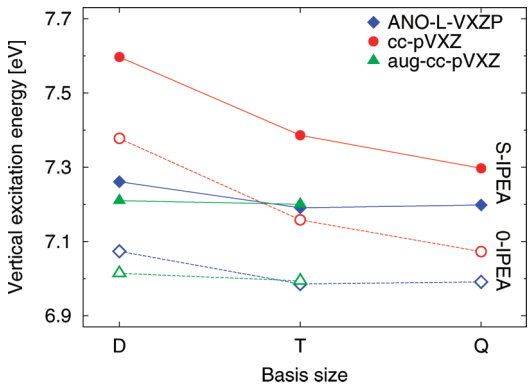

Figure 3. CASPT2 vertical excitation energies of CN3 computed with (S-IPEA) and without (0-IPEA) IPEA shift, and different basis sets. The ground-state MP2/cc-pVQZ geometry is used.

when employing the correlation consistent series, while the ANO energies are well converged when a triple-ζ basis is employed.

The optimal basis set for the present system is a correlation-consistent triple-ζ basis with diffuse augmentation or an ANO triple-ζ basis. Depending on the program, segmented or generally contracted basis sets can be more efficient. As MOLCAS is optimized for generally contracted basis sets, the discussion in the following is based on ANO triple-ζ basis sets. These give CC2 and CASPT2 excitations which are well converged in the basis sets for CN3 as well as for the other molecules (see the SI). In the SI, we also include excitation energies calculated with the correlation consistent Dunning basis sets, more common in CC calculations. The

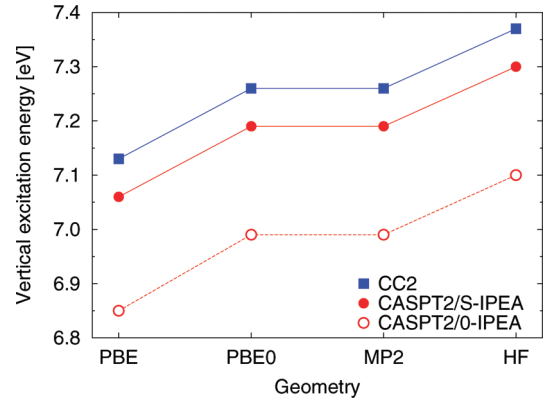

Figure 4. CC2 and CASPT2 vertical excitation energies of CN3 computed on different geometries. The ANO-L-VTZP basis is used.

most efficient choice in segmented contracted basis sets is the recent property-optimized basis sets by Rappoport and Furche.[63] These became available very recently, so we only include a table with the corresponding excitations in the SI.

The dependence of the CC2 and CASPT2 excitation energies on the method employed to optimize the ground-state geometry is shown for CN3 in Figure 4. As in the case of the basis set size, the dependence is most significant for the smallest molecule, CN3, as shown at the CC2 level in the SI. Indepedently of the approach used to compute the excitations and for all chain lengths, PBE and HF geometries give the lowest and highest excitations, respectively, while PBE0 and MP2 geometries are in between. The largest difference between the excitations computed on PBE and HF geometries is 0.24 eV at the CC2 level, as obtained for CN3, and is comparable at the CASPT2 level. The use of PBE0 and MP2 geometries gives very similar excitations with the largest difference of 0.03 eV obtained for CN5. Throughout this work, we use MP2 or PBE0 geometries to reduce the influence of the choice of the ground-state structure on the vertical excitation and focus on the performance of the approach employed to compute the excitations.

3.2. Coupled Cluster Results. For all dyes, we give the convergence of the CC excitation energies with respect to the size of the ANO basis set and the order of the CC expansion in Table 1. As already discussed in section 3.1, the triple-ζ basis set is the most cost efficient choice as an increase to quadruple-ζ only changes the excitation energies by less than 0.01 eV. The CC3 calculations for the largest dye, CN11, are not feasible at the ANO-L-VTZP level, so we also compute the triple-ζ extrapolated CC3 results (exCC3) using eq 3. When available, the CC3 results deviate from their extrapolated counterparts by less than 0.03 eV, and the error in the extrapolation is therefore comparable to the residual basis-set error.

The behavior of the excitation energies at different CC levels reflects the typical convergence of the correlation energy contribution.[26] With the ANO-L-VTZP basis, this convergence is characterized by an increase of less than 0.03 eV when going from CC2 to the full inclusion of doubles amplitudes in CCSD and a decrease of less than 0.14 eV when going from CC2 to CC3. The decrease in excitation energies when going from CC2 to CC3 is larger than the

Table 1. Coupled Cluster Vertical Excitation Energies (eV) for the 1^1B_1 State of the Cyanine Dye Series Computed at the CC2, CCSD, and CC3 Levels with the ANO-L-VXZP Basis Sets[a]

molecule	basis	CC2	CCSD	CC3	exCC3
CN3	D	7.36	7.32	7.27	
	T	7.26	7.29	7.18	7.16
	Q	7.26	7.30	7.18	
CN5	D	5.02	4.98	4.89	
	T	4.97	4.98	4.86	4.84
	Q	4.96	4.99	4.86	
CN7	D	3.83	3.79	3.69	
	T	3.79	3.81	3.68	3.65
CN9	D	3.13	3.09	2.99	
	T	3.10	3.11		2.96
CN11	D	2.66	2.62	2.52	
	T	2.64[b]			2.53

[a] The extrapolated CC3 values (exCC3) are obtained by adding the difference between the double- ζ CC3 and CC2 values to the triple- ζ CC2 results. The ground-state RI-MP2/cc-pVQZ structures are employed. [b] Computed with the RI approximation.

one observed for the corresponding bright state in butadiene (0.04 eV) or in the protonated Schiff base models (0.01 eV).[64,65] The T_1 diagnostic[66] remains lower than the empirical threshold of 0.02, indicating that the Hartree−Fock determinant is a good zeroth-order description of the ground state, and CC2 and CCSD results can therefore be considered reliable.

Further insight into our calculations can be gained by the amount of single- and double-excitation contribution in the CC3 excitation energies. The single-excitation contributions decrease from 89% to 84% when going from CN3 to CN11. The double-excitation contributions increase from 11% to 16% when going from CN3 to CN11. This finding is in line with the growing difference between CC2 and CC3 results upon lengthening of the chain. The correlation energy strongly depends on double excitations for all molecules, and triple excitations contribute more than in the analogous polyenes and protonated Schiff bases. The ground-state correlation energy shows, on the other hand, little dependence on the chain length. For all molecules, 92% of the CC3 correlation energy is obtained already at the CC2 level, and the CC3 correlation energy per electron is identical up to 0.1 mH for all dyes. This finding indicates that electron correlation effects are important mainly in the description of the excitation, for which an accurate description of correlation is therefore essential.

3.3. CASPT2 Results. The choice of the active space significantly affects the CASPT2 energies of the cyanine dyes, particularly of the smallest ones. As shown below, previous calculations[15] employed active spaces that were too small and led to underestimated CASPT2 excitation energies.

We extensively investigated the dependence of the excitations on the choice of the active space, and we give a complete account of our calculations in the SI. In Table 2, we present the most relevant subset of our results where the number of active π orbitals of a_2 and b_2 symmetry included in the CAS is l times the number of heavy atoms. This construction corresponds to l atomic orbitals of p character per heavy atom and produces a series of balanced active spaces. We observe that choosing l equal to 2 offers a good

Table 2. CASPT2 Vertical Excitations (eV) of the 1^1B_1 State Computed with (S-IPEA) and without (0-IPEA) IPEA Shift and with Different CAS(m,n) Expansions[a]

	CAS(m,n)			CASPT2	
molecule	m [a_2, b_2]	n [a_2, b_2]	CASSCF	0-IPEA	S-IPEA
CN3	4 [2, 2]	3 [1, 2]	8.12	6.55	6.90
		6 [2, 4]	7.56	6.99	7.19
		9 [3, 6]	7.63	6.97	7.14
CN5	6 [2, 4]	5 [2, 3]	5.46	4.23	4.62
		10 [4, 6]	5.32	4.46	4.69
		15 [6, 9]	5.33	4.49	4.68
CN7	8 [4, 4]	7 [3, 4]	3.92	3.17	3.56
		14 [6, 8]	3.91	3.30	3.52
		21 [9, 12]	3.96	3.30	3.49
CN9[b]	10 [4, 6]	9 [4, 5]	2.99	2.55	2.92
		18 [8, 10]	3.13	2.59	2.81
CN11[b]	12 [6, 6]	**11 [5, 6]**	2.39	2.10	2.46

[a] All π electrons (m) in the reference are included, and the number of active π orbitals is $n = i + j$, where i and j are orbitals of a_2 and b_2 symmetry, respectively, as specified by the notation [i, j]. The number of active orbitals is a multiple l of the number of heavy atoms as obtained by using l atomic orbitals of p character per heavy atom. We denote in boldface the optimal choice of active space in cost and accuracy for CN3−CN7. For CN9 and CN11, the maximum feasible values of l are 2 and 1, respectively. Additional active spaces not constructed as a multiple of l are listed in the SI. The ANO-L-VTZP basis set and the ground-state RI-MP2/cc-pVQZ structures are employed. [b] Cholesky decomposition with 10^{-8} threshold.

compromise between accuracy and computational cost since the corresponding excitations are always converged to better than 0.05 eV. For the largest dye, CN11, we cannot perform a calculation with l equal to 2, as the use of 22 active orbitals is not feasible. However, the excitation energy of CN11 computed with l equal to 1 is converged within 0.05 eV, as can be seen from the excitations computed with larger CAS dimensions given in the SI.

Our optimal active space must be contrasted to the use of an active space with an equal number of active electrons and active orbitals, as adopted in ref 15. We illustrate the shortcomings of this alternative construction by plotting the excitation of CN3 as a function of the dimension of the active space in Figure 5. The use of a CAS(4,4) space as in ref 15 yields an excitation which is underestimated by as much as 0.4 eV, while the excitation computed with a CAS(4,6) expansion is perfectly well converged. The dependence on the size of the CAS is slightly more pronounced when the zero-order Hamiltonian with no IPEA shift is employed as in ref 15, and as expected, the difference between the excitations computed with and without IPEA shift diminishes with increasing CAS size.

We summarize the CASPT2 excitations for our optimal choice of active space as a function of the ANO basis sets in Table 3. As discussed previously, the use of an ANO triple-ζ basis gives well converged excitations whether one uses the zero-order Hamiltonian with or without the IPEA shift. The excitations computed without the IPEA shift are 0.2 eV lower than the values obtained with the standard IPEA Hamiltonian, independent of the basis. For CN11, the difference between the values computed with and without IPEA shift appears to be larger than for the smaller dyes, and equal to 0.36 eV. The use of larger active spaces would

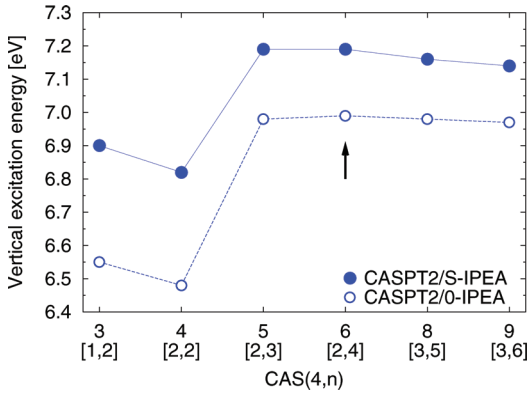

Figure 5. CASPT2 vertical excitation energies of CN3 computed with (S-IPEA) and without (0-IPEA) IPEA shift and with different CAS(4,*n*) expansions. The number of π electrons in the reference configuration is 4. The number of active orbitals is $n = i + j$, and i and j are orbitals of a_2 and b_2 symmetry, respectively, as specified by the label [*i*,*j*]. The arrow indicates a balanced CAS size, which corresponds to the use of two atomic orbitals of p character per heavy atom and represents an optimal compromise in accuracy and cost. The CAS(4,4) chosen in ref 15 is clearly inadequate. The ground-state MP2/cc-pVQZ geometry is used.

Table 3. CASSCF and CASPT2 Vertical Excitation Energies (eV) for the 1^1B_1 State of the Cyanine Dye Series Computed with the ANO-L-VXZP Basis Sets and the Optimal Active Space[a]

		CAS(*n*,*m*)			CASPT2	
molecule	basis	*n* [a_2, b_2]	*m* [a_2, b_2]	CASSCF	0-IPEA	S-IPEA
CN3	D	4 [2, 2]	6 [2, 4]	7.59	7.07	7.26
	T			7.56	6.99	7.19
	Q			7.56	6.99	7.20
CN5	D	6 [2, 4]	10 [4, 6]	5.25	4.53	4.74
	T			5.32	4.46	4.69
	Q			5.32	4.46	4.69
CN7	D	8 [4, 4]	14 [6, 8]	3.85	3.35	3.55
	T			3.91	3.30	3.52
	Q[b]			3.92	3.30	3.53
CN9	D[b]	10 [4, 6]	18 [8, 10]	3.08	2.63	2.83
	T[b]			3.13	2.59	2.81
	Q[b]			3.14	2.59	2.81
CN11	D[b]	12 [6, 6]	11 [5, 6]	2.37	2.13	2.46
	T[b]			2.39	2.10	2.46

[a] A CAS(*n*,*m*) expansion is used to compute the ground- (1^1A_1) and excited-state (1^1B_1) energies, where *n* and *m* denote the number of electrons and molecular orbitals, respectively. The ground-state RI-MP2/cc-pVQZ structures are employed. [b] Obtained with the Cholesky decomposition with 10^{-8} threshold.

however reduce the difference to less than 0.25 eV also for CN11 (see the SI). This finding reflects the fact that CASPT2 excitations computed with the IPEA shift converge faster to the values obtained with larger CAS dimensions.

3.4. QMC Results. In the determinantal component of the Jastrow−Slater wave functions, we choose the active space identified as optimal in the CASPT2 calculations and always optimize at least the Jastrow and linear coefficients in energy minimization within variational Monte Carlo. Other ingredients in the trial wave function may impact the excitation, such as the choice of basis set, the truncation threshold on the CAS expansion, the form of the Jastrow factor, and whether one optimizes also the orbitals in the determinantal component. We investigate the effect of changing these parameters in the wave function and summarize the results in Table 4.

Most tests are performed for the smallest dye, CN3, whose excitation appears to be most sensitive to the features of the wave function. We find that including electron−electron−nucleus terms in the Jastrow factor has little effect on the excitation of CN3. While the VMC excitation slightly increases, the DMC excitation is unchanged by the presence of these additional terms in the Jastrow factor. Therefore, given the higher computational cost of these three-body terms, we only include electron−electron and electron−nucleus correlations in the Jastrow factor for all other dyes. Concerning the basis, we find that the D+ basis leads to excitations which are clearly overestimated in VMC, while T′+ gives converged excitations when compared to the Q′+ values both in VMC and DMC. Even though the shortcomings of a D+ basis are more visible for CN3 than for CN5, we employ a T′+ as the default basis to compute the excitations of all dyes.

More critical for CN3 is the choice of the truncation threshold on the CAS expansion, especially if one does not reoptimize the orbitals. When only the linear coefficients are reoptimized in the presence of the Jastrow factor, the DMC excitation obtained with the full CAS expansion is 0.1 eV lower than the value computed with a threshold of 0.02. If the orbitals are reoptimized, the DMC excitations computed with a full CAS and a truncated expansion become 0.1 and 0.2 eV lower than the corresponding values obtained with CASSCF orbitals, and one recovers the same DMC value when employing the full or truncated CAS expansion. For CN5, the optimization of the orbitals does not significantly affect the excitations, and reducing the truncation threshold on the CAS expansion has a smaller effect on the excitation than for CN3. Therefore, for the larger dyes, we do not reoptimize the orbitals but only make sure we have convergence with respect to the number of configuration state functions included in the determinantal component. For all dyes, we collect the best available QMC results computed with a T′+ and a two-body Jastrow factor in Table 5.

3.5. TDDFT Results. The TDDFT excitations are computed with the PBE, PBE0, and long-range corrected CAM-B3LYP functionals. We also employ the PBE0 hybrid functional in the Tamm−Dancoff approximation (TDA-PBE0) as well as the hybrid functional with a perturbative correction as proposed in Grimme's non-self-consistent B2PLYP scheme.

The TDDFT results are listed in Table 6, where we report the values computed with the ANO triple-ζ basis, which are converged with respect to the basis set to better than 0.02 eV (see the SI). The difference between the PBE and PBE0 functionals is largest for the smallest CN3 dye, where the PBE excitation is 0.22 eV lower than the PBE0 result. With increasing chain length, the PBE and PBE0 excitations approach each other, only differing by 0.06 eV for CN9. For all dyes, the CAM-B3LYP results lie between the PBE and PBE0 results, with PBE giving the lowest excitation. The Tamm−Dancoff approximation and the B2PLYP scheme significantly change the excitation energies of the cyanine

Table 4. VMC and DMC Vertical Excitation Energies (eV) for the 1^1B_1 State of the Cyanine Dye Series[a]

	CAS(*m*,*n*)				CSF/det.				
molecule	*m* [a_2, b_2]	*n* [a_2, b_2]	basis	thr.	1^1A_1	1^1B_1	CASSCF	VMC	DMC
CN3	4 [2, 2]	6 [2, 4]	T′+	0.02	7/11	8/22	7.62	7.58(1)	7.58(2)
			T′+	0.02	7/11	8/22	7.62	7.63(1)	7.58(2)[b]
			T′+	0.02	7/11	8/22	7.62	7.47(1)	7.40(2)[c]
			D+	0.00	57/113	48/144	7.63	7.61(1)	7.50(2)
			T′+	0.00	57/113	48/144	7.62	7.52(1)	7.48(2)
			T′+	0.00	57/113	48/144	7.55	7.52(1)	7.48(2)[d]
			Q′+	0.00	57/113	48/144	7.58	7.51(1)	7.46(2)
			T′+	0.00	57/113	48/144	7.62	7.56(1)	7.47(2)[b]
			T′+	0.00	57/113	48/144	7.62	7.48(1)	7.38(2)[c]
CN5	6 [2, 4]	10 [4, 6]	T′+	0.08	4/7	5/12	5.30	5.21(1)	5.11(2)
			T′+	0.04	8/17	14/38	5.30	5.13(1)	5.05(2)
			D+	0.02	20/51	27/102	5.29	5.13(1)	5.08(2)
			T′+	0.02	22/59	28/106	5.30	5.15(1)	5.04(2)
			T′+	0.02	22/59	28/106	5.30	5.09(1)	5.03(2)[c]
CN7	8 [4, 4]	14 [6, 8]	T′+	0.02	40/111	42/156	3.89	3.90(1)	3.83(2)
CN9	10 [4, 6]	9 [4, 5]	T′+	0.04	13/39	17/42	2.98	3.22(1)	3.11(2)
			T′+	0.02	43/101	65/254	2.98	3.18(1)	3.09(2)
CN11	12 [6, 6]	11 [5, 6]	T′+	0.04	17/54	21/98	2.37	2.68(2)	2.62(2)

[a] A CAS(*m*,*n*) expansion is used to compute the ground-state (1^1A_1) and excited-state (1^1B_1) energies, where *m* and *n* denote the number of electrons and molecular orbitals, respectively. The threshold on the expansion and the corresponding number of CSFs and determinants are also listed. Unless indicated, only the Jastrow and CI parameters are optimized, and the Jastrow factor includes only electron−nuclear and electron−electron terms. The ground-state RI-MP2/cc-pVQZ structures are employed. [b] Including Jastrow e−e−n term. [c] Orbitals optimized including all external orbitals. [d] T′+ basis set with f functions.

Table 5. VMC and DMC Vertical Excitation Energies (eV) for the 1^1B_1 State of the Cyanine Dye Series[a]

	CAS(*m*,*n*)					
Molecule	*m* [a_2, b_2]	*n* [a_2, b_2]	CASSCF	VMC	DMC	
CN3	4 [2, 2]	6 [2, 4]	7.62	7.48(1)	7.38(2)	[b,c]
CN5	6 [2, 4]	10 [4, 6]	5.30	5.09(1)	5.03(2)	[b,d]
CN7	8 [4, 4]	14 [6, 8]	3.89	3.90(1)	3.83(2)	[d]
CN9	10 [4, 6]	9 [4, 5]	2.98	3.18(1)	3.09(2)	[d]
CN11	12 [6, 6]	11 [5, 6]	2.37	2.68(2)	2.62(2)	[e]

[a] For each molecule, we show the best available value from the QMC calculations obtained using the T′+ basis set and a Jastrow factor including electron−nuclear and electron−electron terms. A CAS(*m*,*n*) expansion is used to compute the ground-state (1^1A_1) and excited-state (1^1B_1) energies, where *m* and *n* denote the number of electrons and molecular orbitals, respectively. The threshold on the expansion is also listed. Unless indicated, only the Jastrow and CI parameters are optimized. The ground-state RI-MP2/cc-pVQZ structures are employed. [b] Orbitals optimized including all external orbitals. [c] Thr. of 0.0. [d] Thr. of 0.02. [e] Thr. of 0.04.

Table 6. TDDFT Excitation Energies (eV) of the Cyanine Dye Series Computed with the ANO-L-VTZP Basis Set and Different Functionals[a]

molecule	PBE	PBE0	CAM-B3LYP	B2PLYP	TDA-PBE0
CN3	7.40	7.62	7.55	7.30	8.03
CN5	5.22	5.33	5.26	5.05	5.84
CN7	4.11	4.18	4.12	3.92	4.71
CN9	3.44	3.50	3.44	3.25	4.02
CN11	2.98	3.03	2.97	2.80	3.54

[a] The ground-state PBE0/cc-pVQZ structures are employed.

dyes, as already pointed out in ref 25. The TDA-PBE0 excitations are higher than the PBE0 results by about 0.4 eV for CN3 and 0.5 eV for the other dyes. The B2PLYP excitation energies are 0.25−0.32 eV lower than the PBE0 results.

The excitation of the smallest dye, CN3, shows the strongest dependence on the choice of the functional and, in particular, on the amount of exact exchange included in the functional. While this finding appears to support the suggestion in ref 25 that the self-interaction error is significant for these dyes, we note that the inclusion of exact exchange yields the same excitations as conventional generalized gradient approximations (GGA) for the larger dyes. Therefore, as we discuss in section 4, the discrepancy between TDDFT and correlated methods observed also for the larger dyes cannot be simply attributed to self-interaction error.

Finally, our results follow the general trend observed for a larger set of functionals by Jacquemin et al.,[67] namely, that GGA excitation energies are lower than long-range corrected hybrid-GGA values, while hybrid GGAs give the largest excitation energies. We also note that our excitation energies deviate less than 0.08 eV from those of ref 67, and these small differences can be attributed to the use of different basis sets and ground-state structures.

4. Discussion

In this section, we first focus on the relative performance of the theoretical approaches employed to compute the vertical excitation energies of the cyanine dyes and then discuss their comparison with the available absorption spectra in solution.

4.1. Theoretical Comparison. In Table 7, we summarize our most representative theoretical results for the vertical excitation energies of the cyanine dyes, namely, the extrapolated CC3 excitation energies (exCC3), the CASPT2 values computed with the standard IPEA Hamiltonian (CASPT2/S-IPEA), and the TDDFT energies obtained with the PBE0 functional and the B2PLYP scheme, all computed with the ANO-L-VTZP basis. We also list the best available DMC excitations computed with the T′+ basis set. For an extensive comparison with CC2 or CCSD, CASPT2 with no IPEA shift, and other DFT functionals and the dependence on the

Table 7. Vertical Excitation Energies (eV) for the 1^1B_1 State of the Cyanine Dye Series[a]

Molecule	PBE0	B2PLYP	exCC3	CASPT2	DMC
CN3	7.62	7.30	7.16	7.19	7.38(2)
CN5	5.33	5.05	4.84	4.69	5.03(2)
CN7	4.18	3.92	3.65	3.52	3.83(2)
CN9	3.50	3.25	2.96	2.81	3.09(2)
CN11	3.03	2.80	2.53	2.46	2.62(2)

[a] The CC, CASPT2/S-IPEA, and TDDFT excitations are computed with the ANO-L-VTZP basis set. The best available QMC values obtained with the T′+ basis set are shown.

basis, CAS spaces, and geometries, we refer the reader to the previous sections.

Comparing wave function methods, CASPT2 gives the lowest and DMC the highest excitation energies, while exCC3 falls in between. This energetic order holds for all chain lengths except for CN3, where CASPT2 and exCC3 give almost identical results. The difference between CASPT2 and exCC3 ranges between 0.03 and 0.15 eV, and the differences are smallest for CN3 and CN11. The difference between DMC and exCC3 is of opposite sign and lies between 0.09 and 0.22 eV and decreases steadily from CN3 to CN11.

To establish the relative accuracy of the wave function approaches, we recall that the CASPT2 method is generally quite sensitive to the choice of the zero-order Hamiltonian. For the cyanine dyes, the use of a Hamiltonian with no IPEA shift, as was standard prior to MOLCAS 6.4, yields excitation energies that are on average 0.2 eV lower than the values obtained with the recommended IPEA shift of 0.25 (see Table 3). When the standard IPEA value is adopted, CASPT2 is in better agreement with other wave function methods, indicating that this novel definition of the zero-order Hamiltonian is more accurate and represents an improvement as compared to previous CASPT2 calculations.

Previous CASPT2 calculations of the cyanine dyes by Schreiber et al.[15] are also affected by another problem, namely, an inadequate choice of the CAS space (see Figure 5). The combined effect of the choice of zero-order Hamiltonian and the insufficient CAS dimension explains why the CASPT2 energies of ref 15 are underestimated, in particular for CN3, where their excitation of 6.63 eV must be compared to our value of 7.19 eV. Our excitations of the cyanine dye series should therefore be regarded as more reliable CASPT2 reference values due to the use of the IPEA Hamiltonian and a well converged size of active space.

The agreement between the exCC3 and DMC excitation energies is very satisfactory, with a difference of only 0.1 eV for the largest dyes. The larger discrepancy of 0.2 eV for the smallest dye can be explained by the fact that the high excitation of CN3 is clearly more sensitive to the description of static correlation and other parameters in the wave function. For CN3, the DMC calculations were performed employing the full active space and optimizing also the orbital parameters. The results are stable and further improvement not obvious. When comparing with DFT methods, we will refer to the exCC3 numbers, as they fall in between the CASPT2 and DMC, keeping in mind that the exCC3 excitations, in particular for the smallest dyes, might be slightly underestimated.

The TDDFT excitations computed with the hybrid GGA PBE0 are about 0.35−0.5 eV above the exCC3 results. As discussed in section 3.5, the use of the nonhybrid GGA PBE or the long-range corrected CAM-B3LYP does not lead to a significantly closer agreement with wave function methods. The same holds for the larger number of GGA functionals including the highly parametrized Minnesota functionals tested by Jacquemin et al.[67,68] These findings indicate that a closer agreement with wave function methods can only be obtained by going beyond the GGA and hybrid-GGA levels.

It is evident that the excitation energies of the cyanine dyes are sensitive to the correlation energy treatment. This can be seen in the spread observed among the wave function methods and, at the TDDFT level, from the TDA-PBE0 results. Application of the TDA further deteriorates the agreement with the wave function methods (see Table 6). Within the Tamm−Dancoff approximation, matrix elements that mix excitations and de-excitations are neglected so that the excited state is described by excitations only. It has already been stressed by Grimme and Neese[25] that the present cyanines are one of the rare cases where de-excitations substantially contribute to the excitation energy. Clearly, with the omission of the de-excitations, an important component of correlation energy is neglected.

The only TDDFT approach that significantly improves the agreement with the wave function methods is B2PLYP. The deviation from the exCC3 results ranges between 0.14 and 0.29 eV and increases from CN3 to CN11. The agreement between B2PLYP and DMC is almost perfect for the smaller dyes, and the difference increases to 0.2 for the larger models. Therefore, the discrepancy with either exCC3 or DMC increases for excitations that have a larger double excitation character (as seen in the exCC3 calculations). The improvement given by the use of the B2PLYP scheme comes however at the cost of an increase in computational scaling, the introduction of an additional empirical parameter, and other well-known limitations.[25]

The improved behavior of B2PLYP with respect to GGA or hybrid functionals can be understood from the presence of the additional perturbative correction. The non-self-consistent B2PLYP correction is analogous to the (D) correction in CIS(D) excitation energies, or the MP2 energy correction in the ground state, but computed with Kohn−Sham and not Hartree−Fock orbitals. B2PLYP is therefore an empirical perturbative way to incorporate some double-excitation character into the TDDFT excitation energies. In the ground state, the opposite-spin part of the MP2 energy correction is identical to the first nonvanishing order of the RPA correlation energy, as shown by Eshuis et al.[69] In the excited state, the good performance of B2PLYP is thus an indication that the use of exact RPA correlation may cure the shortcomings of TDDFT in the cyanine dyes by a satisfactory description of double-excitation character. A nonempirical route to incorporate double excitations into TDDFT has been formulated and applied for instance by Cave et al. on polyenes.[70]

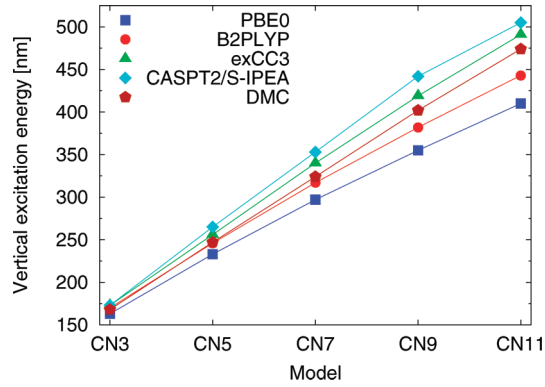

Figure 6. Vertical excitation energies of the cyanine dye series in nanometers. The exCC3, CASPT2/S-IPEA, and TDDFT results are computed with the ANO-L-VTZP basis set. The best available DMC values obtained with the T′+ basis set are shown.

Table 8. Experimental Absorption Maximum (eV) of the Cyanine Dye Series for Different Solutions and Substitutions at the Nitrogen Atoms (R_1, R_2)[a]

	nitrogen termination (R_1, R_2)		
molecule	(H, H)	(H, Me)	(Me, Me)
CN3			5.54[e]
CN5	4.34[c]	4.20,[c] 4.19[d]	3.97,[b] 4.01,[d] 3.96[e]
CN7	3.28[c]	3.15,[c] 3.14[d]	3.01,[f] 2.99,[b] 3.02,[d] 2.98[e]
CN9		2.53,[c] 2.51[d]	2.40,[b] 2.44,[d] 2.39[e]
CN11			1.96,[b] 2.03,[d] 1.98[e]

[a] The dielectric constant and the corresponding experimental temperature are given in brackets. [b] Ref 73, measured in methylendichloride (9.1, 20.0 °C). [c] Ref 74, measured in H_2O (80.4, 20.0 °C). [d] Ref 75, measured in methanol (32.6, 25 °C). [e] Ref 76, measured in methylendichloride (9.1, 20.0 °C). [f] Ref 77, measured in ethanol (24.3, 25 °C).

Finally, as is customary when discussing the cyanine dye series, we show the theoretical excitation energies in nanometers in Figure 6. All methods appear to follow the almost linear behavior traditionally called the vinyl shift.

4.2. Comparison with Experiments. We collect the experimental absorption maxima for comparison with the computed vertical excitation energies in Table 8. The experimental spectra were recorded in different solvents in the presence of ClO_4^- counterions, and all show broad absorption maxima for the lowest excited state. The position of the absorption maxima depends only negligibly on the dielectric constant of the solvent with variations smaller than 0.07 eV. Most experimental values were recorded for cyanine dyes with two methyl substituents on each nitrogen, and the absorption maxima of the methylated species are shifted to lower energies compared to the values of the unmethylated counterparts. The experimental methyl shift is 0.33−0.38 eV for CN5 and 0.26−0.30 eV for CN7 depending on the solvent.

As shown in Table 9, the experimental shifts upon methylation are theoretically well reproduced at the CC2 level with a value of 0.39 and 0.26 eV for CN5 and CN7, respectively, but largely overestimated by TDDFT/PBE0. The methyl shift in the CC2 excitations diminishes from 1.19 eV for CN3 to 0.17 eV for CN11, as expected since the influence of the end groups should vanish in large molecular

Table 9. RI-CC2 and TDDFT/PBE0 Excitation Energy (eV) of the 1^1B_1 State for the Methylated Streptocyanine Dye Series Computed with the ANO-L-VTZP Basis Sets[a]

	CC2		TDDFT/PBE0	
molecule	(H, H)	(Me, Me)	(H, H)	(Me, Me)
CN3	7.26	6.07	7.62	6.00
CN5	4.97	4.58	5.33	4.75
CN7	3.79	3.53	4.18	3.81
CN9	3.10	2.90	3.50	3.23
CN11	2.64	2.47	3.03	2.82

[a] The RI-MP2/cc-pVQZ and PBE0/cc-pVQZ ground-state structures in C_{2v} symmetry are employed for the CC2 and TDDFT calculations, respectively.

Table 10. Vertical and Constrained-Adiabatic Excitation Energies (eV) for the 1^1B_1 State, Obtained with RI-CC2 and the ANO-L-VTZP Basis Sets[a]

	E_{exc} (eV)		
molecule	vertical	adiabatic C_{2v}	Stokes shift C_{2v}
CN3	7.26	6.29	0.97
CN5	4.97	4.64	0.33
CN7	3.79	3.65	0.14
CN9	3.10	3.01	0.09
CN11	2.64	2.58	0.06

[a] Excited-state geometry optimizations are restricted to C_{2v} symmetry. The Stokes shift is the difference between vertical and C_{2v}-constrained adiabatic excitation energy. Relaxing the planarity constraint for CN3 and CN5 indicates that there is no planar minimum.

chains. The geometries of the methylated dyes are obtained in C_{2v} symmetry, but relaxing the symmetry constraint does not change the structure of the dyes, with the exception of CN3, where steric interaction between methyl groups at different nitrogens forces the CN3 dye into a nonplanar structure of C_2 symmetry. Recomputing the excitation energies at the CASPT2 and CC2 levels on the C_2 structure of CN3 only increases the excitations by 0.07 and 0.06 eV, respectively.

The basis for a comparison between computed vertical excitation energies and experimental absorption maxima is the assumption that the transition probability is largest at the ground-state minimum and when the transition is vertical, that is, when ground- and excited-state structures are identical. Examples where these assumptions are not satisfied are numerous,[71,72] but we restrict the discussion here to the validity of the comparison for the cyanine dye series.

The calculation of the absorption spectrum of the cyanine dyes using standard schemes is not possible here since it requires the existence of an excited-state minimum. Relaxing the excited state in C_{2v} symmetry at the CC2 level yields Stokes shifts of almost 1 eV, as shown in Table 10. Further relaxation of CN3 and CN5 without symmetry constraints leads to the highly twisted structures shown in Figure 7. Clearly, absorption spectra based on harmonic potentials in the excited state cannot be calculated for these systems.

The large Stokes shifts given in Table 10 explain the broad absorption maxima in the experiments. Within slight variation of the ground-state geometry, a large number of vibrational states at different energies can be reached if the Franck−Condon region of the excited state is distant from any

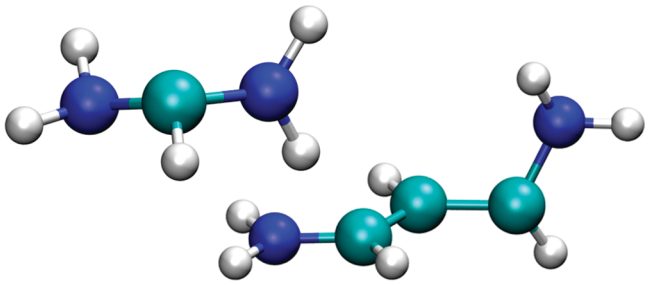

Figure 7. Excited-state minimal geometries of the CN3 and CN5 dyes obtained with RI-CC2 and the ANO-L-VTZP basis sets.

minimum. Moreover, the fact that a relaxed long-lived excited-state structure is most likely nonexistent also increases the likelihood of nonvertical transitions. We therefore conclude that the comparison between the computed vertical excitation energies and the experimental absorption maxima is not reliable, and certainly not suitable to assess the performance of high-level computational methods.

In fact, the direct comparison of calculated vertical excitation energies and experimental absorption maxima shows that CC2 results for the methylated dyes are on average 0.5 eV above the experimental data. The differences range from 0.44 eV for CN11 to 0.62 eV for CN5 and are dependent on the solvent. The deviations of the vertical excitations from the absorption maxima for the methylated species are consistent with the values obtained for the unmethylated dyes. Our CASPT2 excitation energies computed with the recommended IPEA zero-order Hamiltonian and carefully converged dimensions of the active space lie 0.34−0.35 eV above the experimental values. The apparently better agreement obtained in the older work by Schreiber et al. can be explained with their use of an inadequate active space as well as the use of a different zero-order Hamiltonian. The zero-order Hamiltonian used in our work was introduced a few years after the publication of Schreiber's results and is on average more accurate.

In summary, all methods give vertical excitation energies above the experimental absorption maxima with CASPT2 yielding the lowest values but still more than 0.3 eV higher than the experiments. The different wave function approaches yield very similar results, and all lie well above the experimental values. This supports our notion that the experimental absorption maxima correspond to nonvertical transitions. The influence of the solvent and the counterion are not included in our computational description and may further contribute to the discrepancy between theory and experiment.

5. Conclusion

For almost a decade, the simple cyanine dyes studied in this work have represented an intriguing and problematic case for TDDFT and a challenge for the development of new density functionals. The availability of accurate theoretical vertical excitations for these dyes is therefore very important in the assessment of the performance of existing or novel TDDFT approaches. With the present work, we offer carefully benchmarked reference values computed with CASPT2, QMC, CC, and various flavors of TDDFT as an aid for future developments. Our analysis based on such a large variety of excited-state methods gives a broad perspective on the parameters influencing the excited-state description.

We find that previous CASPT2 calculations[15] do not offer a reliable benchmark for the cyanine dyes since the chosen active space was inadequate and led to a severe underestimation of the CASPT2 excitations, with errors as large as 0.6 eV for the smallest CN3 dye. Our CASPT2 calculations are superior to these older studies in the use of the improved zero-order IPEA Hamiltonian and a balanced and well converged choice of the active space. Even though the empiricism introduced by the choice of zeroth-order Hamiltonian renders the assessment of CASPT2 calculations more difficult, the CASPT2 excitations obtained with the recommended IPEA shift appear to be more reliable than those computed without this shift, as the IPEA values are energetically closer to the extrapolated CC3 and DMC results. With our improved CASPT2 vertical excitations, we find that the agreement among all wave function methods is generally quite reasonable, with the largest deviations being observed for the smaller dyes, which appear most sensitive to the treatment of static correlation.

Consequently, the overestimation attributed in the past to TDDFT when comparing to older CASPT2 calculations is now not as severe. Nevertheless, the performance of standard GGA and hybrid GGA functionals is not satisfactory, and our calculations indicate that the discrepancy between TDDFT and wave function methods is due to an insufficient description of double-excitation character at the GGA level. The B2PLYP functional is an empirical scheme to partially incorporate double excitation character, and it significantly improves the description in the cyanine dyes, showing the best agreement with CC3 and DMC results.

Since all wave function methods are in close agreement and the calculations appear rather robust, we consider the corresponding excitations trustworthy. It therefore remains an open question as to why the theoretical results disagree with the location of the absorption maxima in the experimental spectra in solution. Quite surprisingly, we find that the addition of methylation significantly lowers the vertical excitations of the smallest dyes, bringing them in closer agreement with the experimental absorption maxima of the methylated species. Nevertheless, the remaining discrepancy between theory and experiment is quite large, and we attribute it to the presence of nonvertical transitions. In principle, one could prove or disprove this statement by a direct simulation of the absorption spectra. However, these simulations are not straightforward due to the lack of excited-state harmonic potentials and excited-state minima. We find that the relaxation of some of the smaller dyes in planar symmetry leads to Stokes shifts as large as 1 eV, and further unconstrained relaxation yields highly distorted structures that render the reconstruction of the spectra impossible. Clearly, a direct comparison of the experimental absorption maxima and the vertical excitation energies is not reliable and should not constitute the basis for the assessment of theoretical methods.

Acknowledgment. O.V. and C.F. acknowledge the support from the Stichting Nationale Computerfaciliteiten (NCF-NWO) for the use of the SARA supercomputer facilities. The work of R.S. was supported by the Center for Functional Nanostructures (CFN) of the Deutsche Forschungsgemeinschaft (DFG) within project C3.9. We thank Stefan Grimme for his TURBOMOLE implementation of the B2PLYP functional. R.S. acknowledges in-depth discussions with Henk Eshuis; helpful advise from Florian Weigend, Stephan Bernadotte, and Mikael P. Johansson; and critical comments on the manuscript by Filipp Furche.

Supporting Information Available: Assessment of auxiliary basis sets for the RI approximation. Oscillator strengths obtained with RI-CC2. Dependence of the vertical excitation energies on the choice of basis sets, geometry, and other relevant parameters in the different methods (e.g., active space or DFT functional). Dependence of CC2 and CASPT2 vertical excitations of the methylated dyes on the symmetry constraints. Ground-state structures and their dependence on the optimization method and basis set. This information is available free of charge via the Internet at http://pubs.acs.org/.

References

(1) *Light Absorption of Organic Colorants*; Fabian, J., Hartmann, H., Eds.; Springer: Heidelberg, 1980; Vol. 12, p 162.

(2) Strack, D.; Vogt, T.; Schliemann, W. *Phytochemistry* **2003**, *62*, 247.

(3) Mishra, A.; Fischer, M. K. R.; Bäuerle, P. *Angew. Chem., Int. Ed.* **2009**, *48*, 2474.

(4) Mustroph, H.; Stollenwerk, M.; Bressau, V. *Angew. Chem., Int. Ed.* **2006**, *45*, 2016.

(5) Weissleder, R.; Ntziachristos, V. *Nat. Med.* **2003**, *9*, 123.

(6) Würthner, F.; Schmidt, J.; Stolte, M.; Wortmann, R. *Angew. Chem.* **2006**, *118*, 3926.

(7) Ikeda, S.; Kubota, T.; Yuki, M.; Okamoto, A. *Angew. Chem., Int. Ed.* **2009**, *48*, 6480.

(8) Bayliss, N. S. *Q. Rev. Chem. Soc.* **1952**, *6*, 319.

(9) Paci, I.; Johnson, J. C.; Chen, X.; Rana, G.; Popovic, D.; David, D. E.; Nozik, A. J.; Ratner, M. A.; Michl, J. *J. Am. Chem. Soc.* **2006**, *128*, 16546.

(10) Casida, M. E. Time-dependent density-functional response theory for molecules. In *Recent Advances in Density Functional Methods, Part I*; Chong, D. P., Ed.; World Scientific: Singapore, 1995; p 155.

(11) Furche, F. *J. Chem. Phys.* **2001**, *114*, 5982.

(12) Rappoport, D.; Furche, F. Excited states and Photochemistry. In *Time-Dependent Density Functional Theory*; Marques, M. A. L., Ullrich, C. A., Nogueira, F., Rubio, A., Burke, K., Gross, E. K., Eds.; Springer: Berlin, 2006; Lecture Notes in Physics 706, p 337.

(13) Rappoport, D.; Furche, F. *Phys. Chem. Chem. Phys.* **2009**, *11*, 6353.

(14) Fabian, J. *Dyes Pigm.* **2010**, *84*, 36.

(15) Schreiber, M.; Buβ, V.; Fülscher, M. P. *Phys. Chem. Chem. Phys.* **2001**, *3*, 3906.

(16) Hättig, C.; Köhn, A. *J. Chem. Phys.* **2002**, *117*, 6939.

(17) Rappoport, D.; Furche, F. *J. Chem. Phys.* **2007**, *126*, 201104.

(18) Send, R.; Furche, F. *J. Chem. Phys.* **2010**, *131*, 044107.

(19) Cordova, F.; Doriol, L. J.; Ipatov, A.; Casida, M. E.; Filippi, C.; Vela, A. *J. Chem. Phys.* **2007**, *127*, 164111.

(20) Tapavicza, E.; Tavernelli, I.; Rothlisberger, U.; Filippi, C.; Casida, M. E. *J. Chem. Phys.* **2008**, *129*, 124108.

(21) Filippi, C.; Zaccheddu, M.; Buda, F. *J. Chem. Theory Comput.* **2009**, *5*, 2074.

(22) Valsson, O.; Filippi, C. *J. Chem. Theory Comput.* **2010**, *6*, 1275.

(23) Ghigo, G.; Roos, B. O.; Malmqvist, P.-Å. *Chem. Phys. Lett.* **2004**, *396*, 142.

(24) Grimme, S. *J. Chem. Phys.* **2006**, *124*, 034108.

(25) Grimme, S.; Neese, F. *J. Chem. Phys.* **2007**, *127*, 154116.

(26) Schreiber, M.; Silva-Junior, M. R.; Sauer, S. P. A.; Thiel, W. *J. Chem. Phys.* **2008**, *128*, 134110.

(27) Olsen, J.; Jørgensen, P. *J. Chem. Phys.* **1985**, *82*, 3235.

(28) Koch, H.; Jørgensen, P. *J. Chem. Phys.* **1990**, *93*, 3333.

(29) Purvis, G. D.; Bartlett, R. J. *J. Chem. Phys.* **1982**, *76*, 1910.

(30) Christiansen, O.; Koch, H.; Jørgensen, P. *Chem. Phys. Lett.* **1995**, *243*, 409.

(31) Hättig, C.; Weigend, F. *J. Chem. Phys.* **2000**, *113*, 5154.

(32) Hättig, C. *Adv. Quantum Chem.* **2005**, *50*, 37.

(33) Christiansen, O.; Koch, H.; Jørgensen, P. *J. Chem. Phys.* **1995**, *103*, 7429.

(34) Koch, H.; Christiansen, O.; Jørgensen, P.; de Merás, A. M. S.; Helgaker, T. *J. Chem. Phys.* **1997**, *106*, 1808.

(35) Perdew, J. P.; Burke, K.; Ernzerhof, M. *Phys. Rev. Lett.* **1996**, *77*, 3865.

(36) Perdew, J. P.; Burke, K.; Ernzerhof, M. *J. Chem. Phys.* **1996**, *105*, 9982.

(37) Adamo, C.; Barone, V. *J. Chem. Phys.* **1999**, *110*, 6158.

(38) Ernzerhof, M.; Scuseria, G. E. *J. Chem. Phys.* **1999**, *110*, 5029.

(39) Yanai, T.; Tew, D. P.; Handy, N. C. *Chem. Phys. Lett.* **2004**, *393*, 51.

(40) Hirata, S.; Head-Gordon, M. *Chem. Phys. Lett.* **1999**, *314*, 291.

(41) Eichkorn, K.; Treutler, O.; Öhm, H.; Häser, M.; Ahlrichs, R. *Chem. Phys. Lett.* **1995**, *240*, 283.

(42) Weigend, F.; Häser, M.; Patzelt, H.; Ahlrichs, R. *Chem. Phys. Lett.* **1998**, *294*, 143.

(43) *TURBOMOLE 6.2*, TURBOMOLE GmbH: Karlsruhe, Germany, 2010. http://www.turbomole.com (accessed Dec 2010).

(44) DALTON, an ab initio electronic structure program, release 2.0. See http://www.kjemi.uio.no/software/dalton/dalton.html (accessed Dec 2010).

(45) Frisch, M. J.; Trucks, G. W.; Schlegel, H. B.; Scuseria, G. E.; Robb, M. A.; Cheeseman, J. R.; Scalmani, G.; Barone, V.; Mennucci, B.; Petersson, G. A.; Nakatsuji, H.; Caricato, M.; Li, X.; Hratchian, H. P.; Izmaylov, A. F.; Bloino, J.; Zheng, G.; Sonnenberg, J. L.; Hada, M.; Ehara, M.; Toyota, K.; Fukuda, R.; Hasegawa, J.; Ishida, M.; Nakajima, T.; Honda, Y.; Kitao, O.; Nakai, H.; Vreven, T.; Montgomery, J. A., Jr.; Peralta, J. E.; Ogliaro, F.; Bearpark, M.; Heyd, J. J.; Brothers,

E.; Kudin, K. N.; Staroverov, V. N.; Kobayashi, R.; Normand, J. ; Raghavachari, K. ; Rendell, A. ; Burant, J. C.; Iyengar, S. S.; Tomasi, J.; Cossi, M.; Rega, N.; Millam, N. J.; Klene, M.; Knox, J. E.; Cross, J. B.; Bakken, V.; Adamo, C.; Jaramillo, J.; Gomperts, R.; Stratmann, R. E.; Yazyev, O.; Austin, A. J.; Cammi, R.; Pomelli, C.; Ochterski, J. W.; Martin, R. L.; Morokuma, K.; Zakrzewski, V. G.; Voth, G. A.; Salvador, P.; Dannenberg, J. J.; Dapprich, S.; Daniels, A. D.; Farkas, O.; Foresman, J. B.; Ortiz, J. V.; Cioslowski, J.; Fox, D. J. *Gaussian 09*, Revision A.02; Gaussian Inc.: Wallingford, CT, 2009.

(46) Karlström, G.; Lindh, R.; Malmqvist, P.-Å.; Roos, B. O.; Ryde, U.; Veryazov, V.; Widmark, P.-O.; Cossi, M.; Schimmelpfennig, B.; Neogrady, P.; Seijo, L. *Comput. Mater. Sci.* **2003**, *28*, 222.

(47) Roos, B. O.; Andersson, K. *Chem. Phys. Lett.* **1995**, *245*, 215.

(48) Aquilante, F.; Malmqvist, P.-Å.; Pedersen, T. B.; Ghosh, A.; Roos, B. O. *J. Chem. Theory Comput.* **2008**, *4*, 694.

(49) CHAMP is a quantum Monte Carlo program package written by Umrigar, C. J.; Filippi, C. and collaborators.

(50) Burkatzki, M.; Filippi, C.; Dolg, M. *J. Chem. Phys.* **2007**, *126*, 234105.

(51) Filippi, C.; Umrigar, C. J. *J. Chem. Phys.* **1996**, *105*, 213. As a Jastrow correlation factor, we use the exponential of the sum of three fifth-order polynomials of the electron−nuclear (e−n), the electron−electron (e−e), and the pure three-body mixed e−e and e−n distances, respectively. The Jastrow factor is adapted to deal with pseudoatoms, and the scaling factor κ is set to 0.6 au.

(52) Schmidt, M. W.; Baldridge, K. K.; Boatz, J. A.; Elbert, S. T.; Gordon, M. S.; Jensen, J. H.; Koseki, S.; Matsunaga, N.; Nguyen, K. A.; Su, S.; Windus, T. L.; Dupuis, M. J. A. M., Jr. *J. Comput. Chem.* **1993**, *14*, 1347.

(53) Casula, M. *Phys. Rev. B* **2006**, *74*, 161102.

(54) Widmark, P.; Malmqvist, P.; Roos, B. O. *Theor. Chem. Acc.* **1990**, *77*, 291.

(55) Dunning, T. H., Jr. *J. Chem. Phys.* **1989**, *90*, 1007.

(56) Peterson, K. A.; Woon, D. E.; Dunning, T. H., Jr. *J. Chem. Phys.* **1994**, *100*, 7410.

(57) Wilson, A.; van Mourik, T.; Dunning, T. H., Jr. *THEOCHEM* **1997**, *388*, 339.

(58) Weigend, F. *Phys. Chem. Chem. Phys.* **2006**, *8*, 1057.

(59) We take the diffuse functions for the carbon and nitrogen atoms from the aug-cc-pVXZ basis sets in the EMSL Basis Set Library (http://bse.pnl.gov). In the D+ basis, we add the diffuse s and p functions from the aug-cc-pVDZ basis. In the T′+ and Q′+ basis sets, we add the diffuse s, p, and d functions from the aug-cc-pVTZ and aug-cc-pVQZ bases, respectively.

(60) Klopper, W.; Noga, J.; Koch, H.; Helgaker, T. *Theor. Chem. Acc.* **1997**, *97*, 164.

(61) Karton, A.; Taylor, P. R.; Marian, J. M. L. *J. Chem. Phys.* **2007**, *127*, 064104.

(62) Johansson, M. P.; Olsen, J. *J. Chem. Theory Comput.* **2008**, *4*, 1460.

(63) Rappoport, D.; Furche, F. *J. Chem. Phys.* **2010**, *133*, 134105.

(64) Lehtonen, O.; Sundholm, D.; Send, R.; Johansson, M. P. *J. Chem. Phys.* **2009**, *131*, 024301.

(65) Send, R.; Sundholm, D.; Johansson, M. P.; Pawłowski, F. *J. Chem. Theory Comput.* **2009**, *5*, 2401.

(66) Lee, T. J.; Taylor, P. R. *Int. J. Quantum. Chem. Symp.* **1989**, *S23*, 199.

(67) Jacquemin, D.; Perpete, E. A.; Ciofini, I.; Adamo, C.; Valero, R.; Zhao, Y.; Truhlar, D. G. *J. Chem. Theory Comput.* **2010**, *6*, 2071.

(68) Jacquemin, D.; Perpete, E. A.; Scalmani, G.; Frisch, M. J.; Kobayashi, R.; Adamo, C. *J. Chem. Phys.* **2007**, *126*, 144105.

(69) Eshuis, H.; Yarkony, J.; Furche, F. *J. Chem. Phys.* **2010**, *132*, 234114.

(70) Cave, R. J.; Zhang, F.; Maitra, N. T.; Burke, K. *Chem. Phys. Lett.* **2004**, *389*, 39.

(71) Herzberg, G. *Molecular Spectra and Molecular Structure*; Van Nostrand and Reinhold,:New York, 1966, Vol. III, p 173.

(72) Dierksen, M.; Grimme, S. *J. Chem. Phys.* **2004**, *120*, 3544.

(73) Nikolajewski, H. E.; Dähne, S.; Leupold, D.; Hirsch, B. *Tetrahedron* **1968**, *24*, 6685.

(74) Grimm, B.; Dähne, S.; Bach, G. *J. Prakt. Chem.* **1975**, *317*, 161.

(75) Gürtler, O.; Dähne, S. *Z. Phys. Chem., Leipzig* **1974**, *255*, 501.

(76) Malhotra, S. S.; Whiting, M. C. *J. Chem. Soc.* **1960**, 3812.

(77) König, W.; Regner, W. *Ber. Dtsch. Chem. Ges.* **1930**, *63*, 2823.

CT1006295